

# THz Metrology and Instrumentation

Zoya Popović, *Fellow, IEEE*, and Erich N. Grossman, *Senior Member, IEEE*

(Invited Paper)

**Abstract**—This paper gives an overview of measurement techniques used in the THz region of the electromagnetic spectrum, from about 100 GHz to several THz. Currently available components necessary for THz metrology, such as sources, detectors and passives, are briefly described. A discussion of power measurements, vector network analysis and antenna measurements as well as the limitations of these measurements at THz frequencies is given. The paper concludes with a summary of available components and instrumentation for THz metrology at the time of writing.

**Index Terms**—Black body radiation, detectors, network analysis, power, sources, THz.

## I. INTRODUCTION

THE Terahertz region of the spectrum presents a number of difficulties from the metrology perspective due to lack of high-stability sources at sufficient power levels, high noise levels, and high loss of guided structures. As a result, both microwave and optical methods are used; the former are hampered by high loss and difficult packaging and the latter by relatively large wavelengths. A considerable amount of work has been done in various applications unique to this frequency range, and special-purpose instruments have been demonstrated for imaging [1], [2], spectroscopy [3], [4], radioastronomy [5], sensing [6], biology, etc. The reader is referred to other papers in this issue for details on the various applications. In particular, imaging cameras are beyond the scope of this overview paper.

The common sub-system for all of these applications is a low-noise receiver, so in this paper we use a THz receiver as a “driver” for discussing metrology. Fig. 1 shows generic receiver block diagrams, with a few variations noted. Incoming THz frequency electromagnetic radiation is received by an antenna and coupled to either a direct detector with a low-frequency or DC output signal proportional to the incoming intensity (Fig. 1(a)) or a heterodyne receiver (Fig. 1(b)). The incident wave can be modulated as in the case of a radar or communication signal, or unmodulated, as in the case of a radiometer

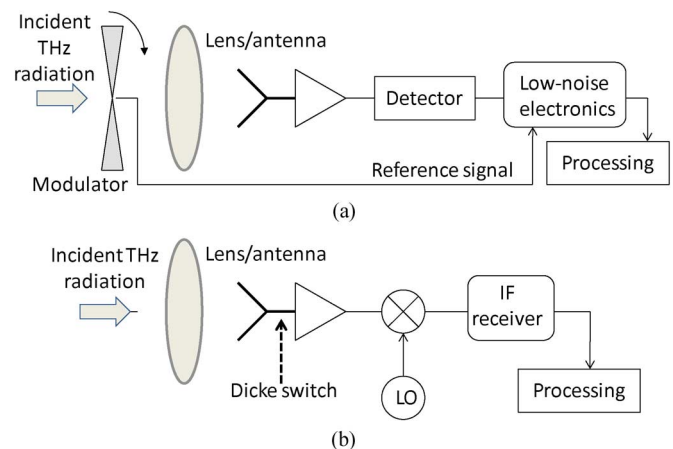


Fig. 1. Block diagram of a THz receiver using (a) direct detection and (b) heterodyne detection. It is common to use modulation at the very front end of the receiver, in order to perform phase-sensitive detection prior to processing, either using an external mechanical chopper or an internal Dicke switch.

or passive imager. The incident radiation can be narrowband (practically single-frequency) or broadband, spanning over a decade, as in e.g. [7]. We will refer to the block diagrams in Fig. 1 throughout the paper as the metrology and instrumentation needed to characterize different receiver components is overviewed. For example, a full description of a direct detection system (Fig. 1(a)), requires well-characterized sources (e.g. blackbodies), calibrated antennas of known coupling efficiency, characterization of noise and sensitivity of detectors, and noise and stability characterization of the entire receiver.

True metrology is an enormous, though highly specialized, branch of science with its own journal [8], vocabulary [9] and national metrology institutes (NIST in the U.S., NPL in the U.K., etc.), to which many in the millimeter-wave and THz development community have had little exposure. The primary purpose of metrology since ancient times [10] has been to support fair commerce, and this underlies the basic concept of traceability to primary standards. However, the existence of any commercial products operating in the THz region, whether components or full instruments, is a fairly recent development compared to other regions of the electromagnetic spectrum. Therefore, a metrological infrastructure similar to that in the optical or microwave regions, including fully documented primary and secondary standards, calibration services, etc., is only beginning to develop [11], [12].

In this paper, we focus on measurement of fundamental quantities (power, scattering parameters, etc.), and especially on the characteristics of systems used to measure those quantities. The

Manuscript received March 23, 2011; revised May 21, 2011; accepted May 30, 2011. Date of current version August 31, 2011. This work was supported in part by the U.S. Department of Commerce.

Z. Popović is with the Electrical, Computer and Energy Engineering Department, University of Colorado, Boulder, CO 80309 USA (e-mail: zoya@colorado.edu).

E. N. Grossman is with the National Institute of Standards and Technology, Boulder, CO 80305 USA (e-mail: grossman@boulder.nist.gov).

Color versions of one or more of the figures in this paper are available online at <http://ieeexplore.ieee.org>.

Digital Object Identifier 10.1109/TTHZ.2011.2159553

TABLE I  
OVERVIEW OF AVAILABLE THZ DETECTORS

DETECTOR	Diode	Quantum	Thermal
<b>Antenna-coupled</b>	Zero-bias [13],[14, 15]	Single-electron tunneling [16]	Micro-bolometer [17],[18]
<b>Surface-coupled</b>	N/A	GaGe/GaAs photoconductive[19]	Pyroelectric [20, 21]
<b>Guided-wave</b>	Schottky diodes [22]	SIS Junction [5]	mm-wave thermistors[23]

paper is intended to present an overview and introduction to this field, and to act as a guide to a microwave or optical researcher who wishes to set up a THz lab. Given this intent, it is impossible to avoid mentioning specific commercial instruments by name. However this in no way constitutes any form of endorsement of such instruments, nor any claim that their quoted specifications are correct. It is also the authors' hope that this paper will help standardize the way certain quantities are measured and reported.

Nearly any THz experiment could be described as a form of instrumentation. However, most are one-of-a-kind, custom-built systems relevant only for their originally envisioned measurements. In this paper on the other hand, the word "instrument" is limited to a measurement system that has been manufactured in quantity, that is calibrated and has published specifications, and that is likely to remain available for a significant time in the future.

The paper is organized as follows:

- Section II describes various components necessary for THz metrology.
- The most fundamental measurements, i.e. scalar power measurements, are described in Section III. DC substitution is overviewed as a fundamental power measurement method and its limitations are discussed, along with power measurement calibration at THz frequencies.
- Section IV is a brief overview of vector network analysis. Various implementations, as well as calibration issues, are discussed.
- Antennas are required for quasi-optical free-space measurements and their characterization at THz frequencies is described in Section V. This includes antenna coupling to Gaussian quasi-optical beams, antenna impedance and radiation pattern measurements.

## II. OVERVIEW OF COMPONENTS FOR THZ METROLOGY

### A. Detectors

A number of detector types are available for the THz frequency range and one possible classification is given in Table I. The detectors are characterized by fundamental physical operation (diode, quantum, thermal) and by coupling type, i.e. antenna, surface, or waveguide. ("Diode" detection in this context denotes the existence of macroscopic THz currents, and is unrelated to the IR usage of "photodiode".) Details on each type are given in the references provided in the table, and an example of an antenna-coupled microbolometer is shown in Fig. 2.

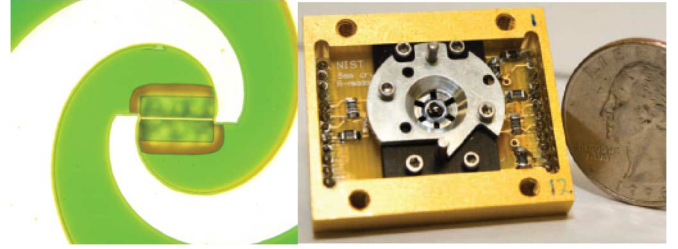


Fig. 2. Optical micrograph of a Nb microbolometer coupled to a spiral antenna on Si (left) and substrate Si lens and readout electronics (right).

For a realistic (noisy) detector, the RMS noise power is described by the noise-equivalent power (NEP) and is obtained by referring the noise to the input:

$$\text{NEP} = \frac{i_n}{\Re_I} \text{ and } \text{NEP} = \frac{v_n}{\Re_V}$$

where  $i_n, v_n$  are noise current and voltage spectral densities (in  $V/\sqrt{\text{Hz}}$ ), and  $\Re_I$  and  $\Re_V$  current and voltage responsivities, defined by the THz power incident (not absorbed) at a reference plane and the open-circuited voltage ( $V$ ) and short-circuited current ( $I$ ) by

$$\Re_V = \frac{V}{P} \text{ and } \Re_I = \frac{I}{P}.$$

Assuming the voltage noise is white around the detection frequency, the minimum detectable power scales as  $T^{-1/2}$  where  $T$  is the integration time. The standard deviation of the power measurement is given by

$$\sigma^2 = \text{NEP}^2/(2T). \quad (1)$$

In other words, a one-second integration time corresponds to a 1/2 Hz equivalent noise bandwidth.

We regard NEP as the fundamental figure of merit for an antenna-coupled detector. Noise-equivalent temperature difference (NETD), which is commonly used for IR detector or camera characterization, by contrast refers to a complete system, since it involves assumptions about the passive quasi-optical parts of the systems. The two are related by noting that antenna-coupled detectors couple (by definition) to a single spatial mode of the electromagnetic field, meaning a single polarization and a single diffraction-limited spot. Therefore, the power coupled from a blackbody at temperature  $T$  (in the Rayleigh-Jeans limit,  $hf \ll kT$ ) is simply  $kTB$ , where  $B$  is the pre-detection bandwidth. The relation between NEP and NETD is then

$$\text{NEP} [\text{W}/\sqrt{\text{Hz}}] = kB \text{ NETD} \sqrt{2\tau}$$

$$1 \text{ pW}/\sqrt{\text{Hz}} = 2.8 \text{ K} \left( \frac{B}{100 \text{ GHz}} \right) \sqrt{\tau \times 30 \text{ fps}} \quad (2)$$

where  $\tau$  is the integration time per frame. It is important to specify this integration time (often standardized at 1/30 s, as in the numerical example) and the location of the reference plane in describing THz detector performance.

TABLE II  
OVERVIEW OF AVAILABLE THz SOLID-STATE SOURCES

	100 – 300GHz	0.3 – 1 THz	1 – 3 THz
<b>Waveguide</b>	Gunn [29] or IMPATT [30] diodes with or w/o multipliers	Multipliers [26],[31]	Multipliers [26],[32]
<b>Planar</b>	Transistor-based [33]	N/A	N/A
<b>Antenna</b>	Photomixers [34]	Photomixers [34] [35]	Photomixers [34] [35]
	Grid multipliers [36],[37]		

Typical NEPs for pyroelectrics are around  $1 \text{ nW}/\sqrt{\text{Hz}}$ , and around  $10\text{--}100 \text{ pW}/\sqrt{\text{Hz}}$  (from 200 GHz and 1 THz) for a zero bias diode. NEPs of antenna-coupled room-temperature micro-bolometers are also in the  $10\text{--}100 \text{ pW}/\sqrt{\text{Hz}}$  range. NEPs of cryogenic detectors for radio-astronomy have been reported below  $10^{-19} \text{ W}/\sqrt{\text{Hz}}$  [24] far below the background limit for 300 K backgrounds.

### B. Sources

The limited existing THz sources are summarized in Table II. Higher power tube-based sources, e.g. [25], are not extensively overviewed in this paper since they are not often used in metrology. Gunn and IMPATT fundamental frequency sources are available commercially with up to 150 mW output power at W-band and 30 mW at 120–140 GHz, but they lack sufficient power to drive the highest frequency multiplier chains (currently extending above 2 THz), and moreover require mechanical tuning. Instead, a lower frequency oscillator, such as a DRO, YIG oscillator, or synthesizer, is typically followed by a W-band power amplifier, which in turn is followed by a high frequency multiplier chain. This provides power generation, currently up to 2.7 THz, with standard sized, dominant mode, waveguide outputs [26]. Planar (monolithic) transistor-based sources have recently been pushed into the G-band [27] with 50 mW of output power obtained by on-chip combining.

Antenna-coupled photomixers, first developed in the mid-1990s [28], are unsurpassed as sources to cover ultra-wide bandwidths ( $\sim 100 \text{ GHz}$  to  $\sim 2 \text{ THz}$ ) in a single sweep, but their power levels are quite low, typically a microwatt or less. They are commercially available from multiple vendors and are widely used spectroscopic tools.

Another type of free-space coupled source is the multi-mode grid multiplier which multiplies the frequency of an incident plane wave in transmission or reflection [37]. A metal grid loaded with diode multiplier elements allows large input power levels since the power is distributed among the diodes.

Other active devices have been demonstrated well into the THz range, for example in [38], a 2.5-THz Schottky diode mixer is demonstrated which combines conventional machined metallic waveguide with micromachined monolithic GaAs circuitry to form a room-temperature planar diode receiver. An InP MMIC low-noise amplifier with 16 dB gain at 340 GHz was also demonstrated in 2007 [39], and extended to 480 GHz [40] paving the way to integrated THz circuits, reviewed in more detail in another paper in this issue.

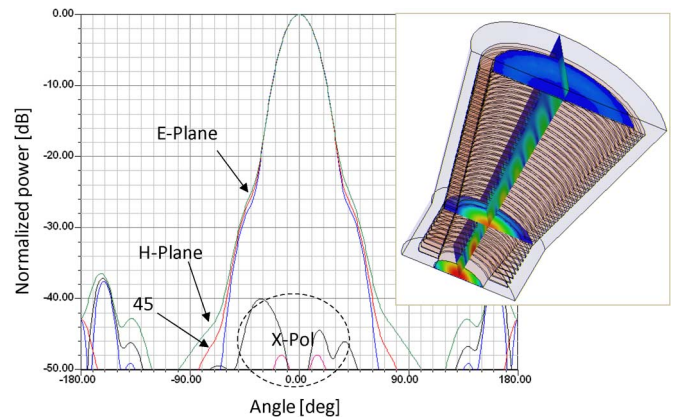


Fig. 3. Corrugated (scalar) horn antennas with very similar E and H plane patterns [48] and waveguide feeds can be designed and manufactured using various techniques, e.g. micromachining or electroforming [43].

THz spectroscopy was first developed using high-resolution frequency-domain techniques extended from the microwave region, typically on gas phase samples with narrow lines. This is still an area of active work [41]. However, the remarkable expansion of THz spectroscopic applications that began in the mid 1990s was primarily due to the development of THz time-domain sources based on photoconductive switches and ultra-fast lasers [42]. This type of source and its applications have been described in many reviews, see e.g. [6]. The last five years have witnessed a resurgence in all-electronic source approaches, largely because of advances in high-speed (HEMT and HBT) transistors (see [33]). The present paper's emphasis partly reflects this current focus on transistor and diode-based sources and instruments at THz frequencies.

### C. Passive Components

A number of passive components are needed for THz measurements, both in waveguide and quasi-optical form, and are available from too many sources to include all. Low-loss waveguides in standard bands are available from a number of vendors, e.g. [43], as well as various waveguide components such as loads, waveguides, isolators, filters, couplers, etc. Tapers between standard waveguide sizes are common [44], and provide access to components embedded in overmoded waveguide. Interestingly, it has been shown that overmoded waveguide can have extraordinarily low loss [45].

Quasi-optical components such as scalar horns and lenses enable high-quality Gaussian beams for quasi-optical instruments [46], [47]. Corrugated horns such as the one shown in Fig. 3 can be designed to have very similar beams in the two planes with low cross-polarization, and with very high coupling efficiency to a Gaussian beam.

There are always new technologies which hold promise for high-quality THz components. One such technology is the PolyStrata from Nuvotronics, LLC [49]. Recent advances in fabrication techniques for micro-electromechanical systems (MEMS), including surface and bulk micromachining, provide tools that make it possible to produce miniaturized TEM rectangular coaxial lines with heights from  $50 \mu\text{m}$  to  $800 \mu\text{m}$ . The electrical properties of these air-filled lines that make them

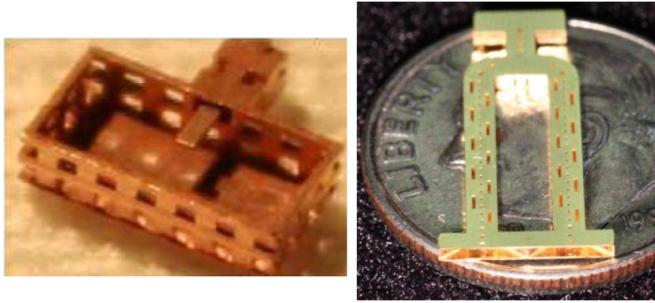


Fig. 4. Left: Recta-coax to WR-10 adapter fabricated in the PolyStrata process by Nuvotronics [49]. Right: Two G-band slotted-waveguide scanning arrays with horn terminations fabricated in the same process (copper with gold coating). Photographs courtesy Nuvotronics, LLC.

attractive for millimeter-wave and broadband applications include ultra-low dispersion with a dominant TEM mode up to 400–500 GHz, depending on the size of the coaxial line and its characteristic impedance [50] and low loss (0.1 dB/cm measured up to 50 GHz). The loss increases due to skin effect and surface roughness of the center conductor, with an estimated loss of 0.22 dB/cm for 0.1  $\mu\text{m}$  rms roughness at W-band. In addition, the coupling between neighboring lines is very low, and a wide range of characteristic impedances is possible. A large number of millimeter-wave (through V-band) narrow-band components such as resonators, hybrids, and antennae were demonstrated with this technology (Fig. 4). A WR10 waveguide to coaxial line transition has been demonstrated at W-band [51], and recently waveguide frequency-scanning slot arrays were demonstrated in G-band in the same process [52] shown in Fig. 4, and with an estimated loss of 0.06 dB/cm for the dominant mode.

### III. POWER MEASUREMENTS

In the mm-wave/THz region, absolute power measurement is a necessary adjunct to the development of sources. Power measurements in the THz frequency range have been approached from the optical/IR and the microwave sides: absolute power measurements in free space (absolute radiometry), e.g. [53], [54], and waveguide-based power measurements, e.g. [55]. Power measurements for high power tube sources have primarily been based on custom, flowing-fluid (usually water or alcohol) calorimeters, e.g. [56], [57].

Virtually all absolute power measurements are based on the principle of *electrical substitution radiometry* (ESR), which is often taken as synonymous with absolute radiometry. This is a bolometric technique, in which the basic elements of a bolometer, namely a thermometer and an absorber, are supplemented with an electrical heater, typically a simple resistor. The thermometer's response due to power deposited in the absorber is compared to its response to DC power deposited in the electrical heater. The latter is determined to high accuracy by monitoring the voltage and current delivered to the heater. The substitution can be done in a closed feedback loop for faster measurements. A remarkable, even inspirational, set of ESR measurements, are the IR cryogenic radiometry done in



Fig. 5. Four commercial power meters in common use in the 0.1–10 THz band. From left: Agilent W8486A, VDI (Erickson) PM4, Thomas-Keating THzPM, and Scientech AC2500.

the mid-1980s at NPL [58], and used in the most accurate determination of the Stefan–Boltzmann constant [59]. This spawned an entire generation of cryogenic radiometers [60] that form the basis for modern high-precision IR power measurement and international standards.

For general laboratory (i.e. non-metrologic) uses, the early default method for measuring THz power was simply to use a commercial radiometer originally developed for IR or microwave wavelengths, applying if possible, a correction factor to account for imperfect performance of the absorber. The Scientech 362 calorimeter, originally modeled after an NBS design [61], is probably the most prominent example of such an IR sensor pressed into THz use; the Agilent W8486A W-band sensor [23] has likewise been pressed into use at (somewhat) higher frequencies. However, since the mid-1990s instruments specifically designed for THz frequencies have been available, such as those developed by Erickson Instruments [62]–[64] and Thomas Keating Ltd. [65] (see Table IV and Fig. 5). A critical aspect of the former is that its input is coupled through WR-10 waveguide (inner dimensions  $2.54 \times 1.27$  mm), in a standard UG-387/UM flange.

At frequencies above 120 GHz, this waveguide is over-moded, and at the higher frequencies where it is often used (say, above 500 GHz), the number of propagating modes is large. Common practice for measuring power in single-mode waveguide is to insert a tapered, rectangular-waveguide, transition between the single-mode waveguide's output flange and the instrument's WR-10 input flange. Such transitions are commercially available, and their performance is described in a useful Virginia Diodes application note [44]. The instrument's absorber is designed to provide high absorption for any mode that may be propagating down the waveguide.

Another recently developed waveguide-based power meter, also using a dual-load design, [66] has been measured against a Russian power standard [67] over the 110–170 GHz range. Separately, as part of the Herschel satellite development, a power meter was built [68], and in combination with a FIR molecular gas laser, used for measurements of mirror emissivity. This power meter, like the Scientech AC2500 and other IR sensors

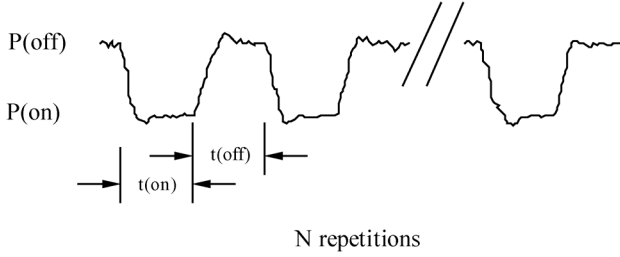

 Fig. 6. Substitution power  $P(t)$  versus time for a typical ESR measurement.

 TABLE III  
 SUMMARY OF MEASUREMENT VARIANCE FOR ESR PROTOCOLS

	$S_p(f)=S_0$	$S_p(f)=S_0(f_0/f)$	$S_p(f)=S_0(f_0^2/f^2)$
$w_0$	$S_0/(2T)$	Diverges	Diverges
$w_1$	$2S_0/T$	$(4\ln 2)S_0f_0$ $\cong 2.77 S_0f_0$	$(2\pi^2/3) S_0f_0^2T$ $\cong 6.58 S_0f_0^2T$
$w_2$	$2S_0/T$	$3\ln(27/16)(S_0f_0)$ $\cong 1.57S_0f_0$	$(\pi^2/2) S_0f_0^2T$ $\cong 4.93 S_0f_0^2T$
$\sigma_{Allan}^2(T)$	$S_0/(2T)$	$(2\ln 2)S_0f_0$ $\cong 1.39S_0f_0$	$(2\pi^2/3) S_0f_0^2T$ $\cong 6.58 S_0f_0^2T$

used for THz measurements, is based on absorption in a special, broadband absorbing coating applied to a substrate (in this case a 25 mm diameter aluminum disk).

### A. Metrics

The NEP is the important statistical figure of merit when the amount of time available to perform a measurement is limited, fixed, and shorter than the timescales of low-frequency fluctuations or drifts. This is the situation in video imaging for example, where the available measurement time cannot exceed the frame period (1/30 s for most video standards). Since the NEP is the power spectral density of noise, it is most meaningful when the noise is white in a bandwidth around the frequency of interest.

In this case, averaging improves the noise, and the standard deviation  $\sigma$  of the final power measurement is reduced by the square root of the number of measurements [see (1)]. A common rule of thumb for the “useful” bandwidth of a detector or instrument is that between its 1/f knee and its 3 dB rolloff in responsivity. However, when more time is available for a measurement than the inverse of its 1/f knee frequency, then low-frequency (1/f) noise and drifts in the instrumentation limit the statistical uncertainties.

### B. Substitution Error and Allan Variance

Because high accuracy radiometers are frequently slow (seconds), dealing with drift and 1/f noise is critical to ensuring accurate measurements. Fig. 6 shows a differential measurement, where the radiometer output is averaged over periods with an open shutter (on) and a closed shutter (off) and then subtracted.

Let the power recorded by the radiometer be  $P(t)$  and the power spectral density (PSD) of its fluctuations be  $S_P(f)$ . A windowing function, referred to as the “measurement protocol” describes how long the signal is averaged in the on and off states,

how many cycles are measured, the dead time, etc. This windowing function  $w(t)$  defines a filtered signal  $Q(t)$  by

$$Q(t) = \int_{-\infty}^t P(t')w(t-t')dt'.$$

The result of the measurement is the value of  $Q(t)$  at the end of the measurement period. It is useful to consider three simple measurement protocols:

$$w_0(t) = \begin{cases} 1/T, & 0 < t < T \\ 0, & \text{elsewhere} \end{cases}$$

$$w_1(t) = \begin{cases} 2/T, & 0 < t < T/2 \\ -2/T, & T/2 < t < T \\ 0, & \text{elsewhere} \end{cases}$$

$$w_2(t) = \begin{cases} 2/T, & 0 < t < T/4 \\ -2/T, & T/4 < t < 3T/4 \\ 2/T, & 3T/4 < t < T \\ 0, & \text{elsewhere} \end{cases}$$

The first, which we refer to as “on”, consists of simply averaging the radiometer output over time  $T$ . We refer to  $w_1(t)$  as “on-off” and to  $w_2(t)$  as “on-off-off-on”. All three protocols average for a total time of  $T$ ;  $w_1$  corrects for a constant offset but not a linear drift, while  $w_2$  corrects for both.

The basic signal-processing result is that the variance  $\sigma^2$  in a measurement of  $Q$  defined above is given by

$$\sigma^2 = \int_0^{\infty} S_Q(f)df = \int_0^{\infty} S_P(f) |\tilde{w}(f)|^2 df \quad (3)$$

where  $\tilde{w}(f) = \int_{-\infty}^{\infty} w(t)e^{2\pi i f t} dt$ . The statistical uncertainty for the various measurement protocols, in the presence of white,  $1/f$ ,  $1/f^2$  or other forms of noise spectrum, can be calculated as summarized in Table III.

Most detector and instrument PSDs can be well described as superpositions of white,  $1/f$ , and possibly  $1/f^2$  power laws. Fitting a measured PSD to such a superposition yields the coefficients  $S_0$  and  $f_0$  for each component. Since (3) is linear in  $S_P(f)$ , the numerical coefficients listed in Table III can then be used to provide a rigorous numerical value for the uncertainty in a measurement made by protocols  $w_1$  or  $w_2$ .

In the 1970s and 1980s, the concept of Allan variance was developed [69], [70] to address similar issues in high accuracy time and frequency metrology. Its two chief advantages are the simplicity of its definition and calculation, and the fact that, unlike the classical variance, it converges even in the presence of  $1/f^n$  fluctuations, for  $n \geq 1$ . It became clear however, that its usefulness is much broader than simply in time and frequency metrology, and it soon began to be applied to radiometry [71]. Its use is now fairly widespread in the instrumentation development communities for astronomy [72], microwave remote sensing [73], [74], and metrology [74], [75]. It does not seem to have propagated to commercial THz instrumentation manufacturers yet, although that is certainly a desirable and likely outcome in the reasonably near term.

### C. Systematic Errors in THz Power Measurements

In practice, the reproducibility with which signals can be coupled into instruments usually dominates the uncertainty of THz measurements. This “reconnection uncertainty” is a well recognized problem for waveguide components, and accounts for the considerable effort currently being made to improve the interconnection technology, either through incremental improvements to the standard UG387 flange [76], [77], or with more drastic changes such as sleeve-based interconnection [78] similar to fiber optic connectors. The corresponding uncertainty in free space radiometric measurements arises from uncertainty in the optical throughput or etendue (area times solid angle) presented to the instrument. In a precision measurement [59], great care is taken to control the baffle dimensions that determine throughput [79], and to correct for diffraction effects [80], [81], and uncertainties at or below the 100 ppm level ( $-40$  dB) are possible. This is greatly superior to the control possible even with improved versions of standard UG-387 waveguide interconnects. For this reason, it seems that implementation of *fundamental* THz power standards ought to begin in free space.

### D. Calibration Standards for THz Power Measurements

Between 110 GHz and the long-wave IR (roughly 10 THz), no national standards exist, neither source-based nor detector-based (see [82]), for power or any other electromagnetic quantity, although plans to develop such standards are being made at several national metrology institutes [11], [83], [84]. Researchers and technology developers therefore fall back onto the physical basis for radiometric calibrations, which in the THz region is the Planck (blackbody) radiation law:

$$L(f, T, \varepsilon) = \varepsilon \frac{2hf^3}{c^2} \frac{1}{e^{hf/kT} - 1}$$

describing the *spectral radiance* (power emitted per unit area, per unit solid angle, and per unit frequency) emitted at frequency  $f$  by a surface with temperature  $T$  and emissivity  $\varepsilon$ . (Physical constants  $h$ ,  $k$ , and  $c$  have their usual meanings.) Blackbodies used for the calibration of radiometers must have a temperature that is well controlled and an emissivity as close to unity as possible, since any power viewed by the radiometer that is not emitted, must be transmitted through or reflected off the blackbody’s surface from its surroundings, which have an uncontrolled radiometric temperature. This largely reduces to a question of material properties and geometry.

Low reflectivity materials are also required for constructing anechoic chambers and radar cross-section (RCS) ranges. A archetypal example of a highly engineered THz blackbody calibrator is that developed for the FIRAS spectrophotometer [85], the instrument that provided definitive measurement of the cosmic microwave background spectrum. Its emitting surface was cast from a common microwave absorbing material, Emerson and Cuming CR-series “Eccosorb”, an iron-loaded epoxy whose reflectivity had earlier been carefully measured [86] across the band of interest. Such microwave absorbers are still widely used in the terahertz band, in castable form, foam (e.g. AN-72), and other forms.



Fig. 7. Left: “Witches hat” blackbody is injection formed by Thomas Keating Ltd. in absorbing plastic to give  $s_{11} = -80$  dB at 100 GHz. Right: Aqueous blackbody, or “THz trap”, made of Styrofoam and water kept at a monitored temperature (NIST-Boulder).

Anechoic materials specifically designed for THz frequencies have been developed at the Univ. of Massachusetts’ Submillimeter Technology Lab [87] and at Thomas Keating Ltd., and both are available commercially. The former include both narrowband “Dallenbach” surfaces based on metallic paints, as well as more broadband structures based on absorber-loaded silicone. Extensive comparative characterization is described in [87], including 200–3000 GHz FTS measurements, and angle-dependant measurements at 584 GHz.

Similar comparisons have been made at 310 GHz in [88], at 650 GHz in [89], and at spot frequencies over 200–600 GHz in [90]. Some of these comparative studies have also included samples of wool or synthetic carpet. Its THz anechoic performance is quite respectable, which is important for cases where large areas need to be covered, and cost is therefore a significant consideration. Absorbing coatings developed for the Herschel instruments, consisting of SiC-loaded Stycast (widely used at microwave frequencies) are described in [91].

Geometric optics (ray-tracing) can be used to predict the position and direction of stray (THz) waves assuming that any residual reflectance is specular. The geometry can then be optimized, resulting in the linearly wedged, pyramidal, or conical geometries of many of the absorbers cited above. The simple blackbody load described by Siegel [92], based on a SiC foam embedded in Eccosorb resin, includes a hinge to allow for adjustment of the wedge angle. An early THz blackbody [93] embodied these same geometric principles. More recent THz blackbodies have usually been designed around specific satellite or atmospheric remote sensing missions, e.g. [94], which is used on several ESA airborne and balloon-borne instruments with a return loss as low as  $-70$  dB. A simple low-cost blackbody that relies on water as the absorbing medium [95] has also been developed, based on IR standards-grade “optical traps”, Fig. 7. It is currently under evaluation as a NIST-traceable reference, and prototype versions have already been distributed to over 20 early adopters worldwide.

## IV. NETWORK ANALYSIS

Vector measurements of  $S$ -parameters using microwave network analyzers have been progressively extended from 110 GHz into the THz frequency range by several companies working with the major microwave network analyzer manufacturers (see Section VI). In the late 1980s, Goy (ABMillimetre) demonstrated stand-alone network analyzers operating well above W-band [96], [97]. At the time of writing of this paper,



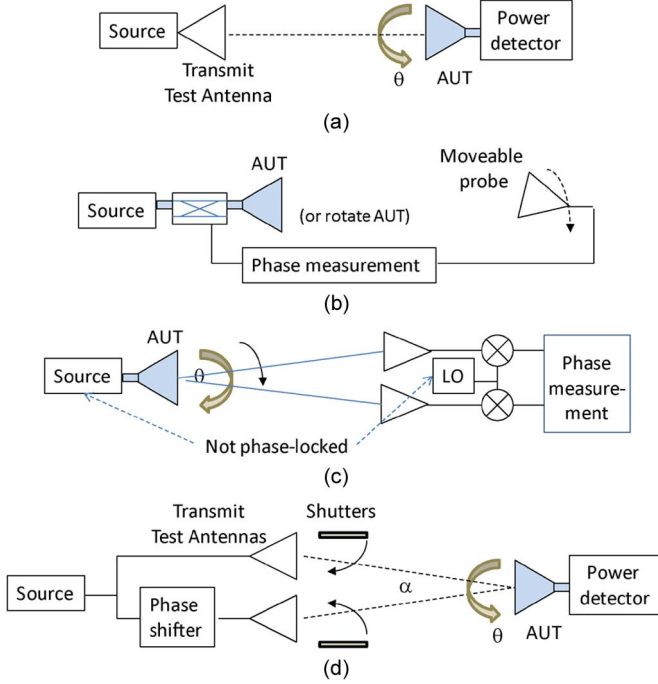


Fig. 11. Block diagram of several antenna radiation pattern measurement approaches. (a) Power pattern measurement obtained by rotating the AUT in reception. (b), (c) Amplitude and phase measurement techniques using a phase sensitive receiver. (d) Interferometric (“holographic”) amplitude and phase measurement method. A VNA is a natural way to implement (b) and (c) [107]. The gradient of the phase is measured in (c) and (d) and subsequent integration is needed to obtain the phase pattern.

the Gaussicity can be found from an overlap integral of the measured radiation pattern  $E_A$  and the Gaussian beam profile  $E_G$ :

$$G = \frac{\int_S |E_A(x, y)|^2 |E_G(x, y)|^2 dS}{\sqrt{\int_S |E_A(x, y)|^2 dS \cdot \int_S |E_G(x, y)|^2 dS}}$$

For the measured pattern of a spiral antenna on a Si substrate, integrated with a microbolometer as shown in Fig. 12, the coupling to the Gaussian beam optics is found to be  $G = 86\%$  at 650 GHz and 82% at 238 GHz [106]

Two techniques for measurement of phase patterns on microwave antennas are illustrated in Fig. 10(b) and (c). These involve the use of a phase-sensitive receiver to monitor the phase difference between the illuminating source (radiated through the AUT) and a probe antenna which is rotated about the AUT (b), or between the AUT and a fixed probe antenna while both are illuminated with a plane wave and the AUT is rotated (c). The difficulty with extending either technique to higher frequency is the need to pass the high frequency signal through movable cables or a rotary joint without introducing spurious angle-dependent phase delays.

In the setup illustrated in Fig. 11(d), the rotatable AUT is operated in reception and two phase-coherent interfering beams are incident at its aperture. This technique is based on [108]. By measuring the received power for each incident wave alone ( $P_1$  and  $P_2$ ) and then for the coherent sum of the two beams ( $P_{TOT}$ ), the phase difference between the waves,  $\phi$ , generated in the AUT can be easily derived and is the gradient of the antenna

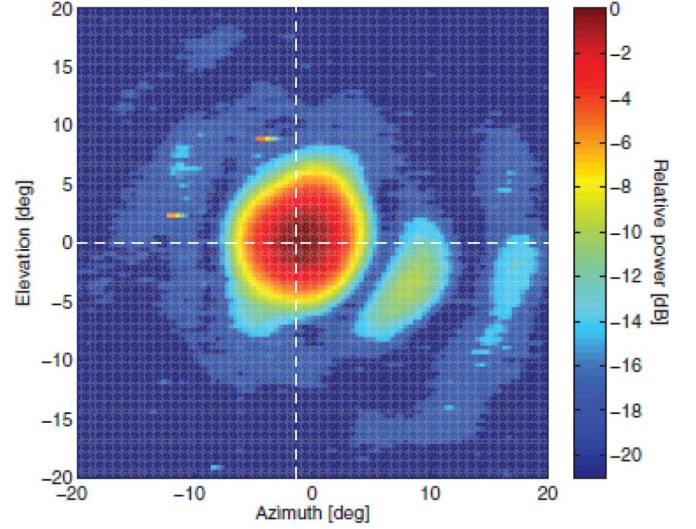


Fig. 12. Measured antenna and microbolometer power-only pattern at 650 GHz. This antenna is coupled to a Gaussian beam and has a Gaussicity of 86% [106].

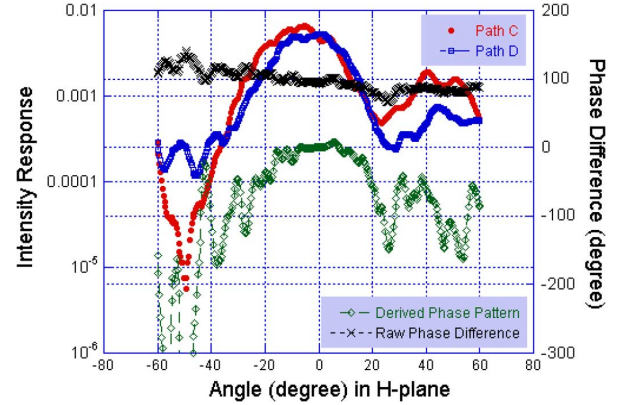


Fig. 13. Representative phase pattern measured at W band using the method from Fig. 11(d) [109]. The power density at W-band at the AUT plane is approximately  $1 \mu\text{W}/\text{mm}^2$ .

phase pattern measured in reception. For an interferometer, the combined detected power is given by

$$P_{TOT} = P_1 + P_2 - 2\sqrt{P_1 P_2} \cos \phi$$

and the phase is obtained from purely power measurements as

$$\phi = \arccos \left[ \frac{P_{TOT} - P_1 - P_2}{2\sqrt{P_1 P_2}} \right].$$

Such a setup has been implemented in a compact automated antenna range, and validated on a previously reported planar slot-ring antenna at 95 GHz [109]. A set of Gunn oscillators optimized for broad tuning range provides the incident power. An example radiation pattern obtained using this setup is shown in Fig. 13.

## VI. DISCUSSION AND CONCLUSIONS

As mentioned above, no national standards for THz power or radiometric temperature exist between 110 GHz and 10 THz at present. There is however an enormous heritage of such standards in the thermal IR region, much of it based on (filtered) blackbodies. It is therefore natural to imagine an infrastructure

TABLE IV  
OVERVIEW OF AVAILABLE THz INSTRUMENTS

COMPANY	Model	Measurement	Frequency*	Coupling	Comments**
VDI/Erickson <a href="http://vadiodes.com/">http://vadiodes.com/</a>	PM4	Power	0.1 - >2 THz	WR-10 waveguide (1.27 x 2.54 mm)	10 nW "typ. RMS noise"
Thomas Keating Ltd. <a href="http://www.terahertz.co.uk/">www.terahertz.co.uk/</a>	Absolute THz Power Meter	Power	0.03 - >3 THz	Free space >30 mm diam.	5 $\mu$ W/Hz <sup>1/2</sup> "typ. NEP"
Scientech Inc. <a href="http://www.scientech-inc.com">www.scientech-inc.com</a>	Astral AC 2500	Power	8 – 1200 THz	Free space 25 mm diam.	10 $\mu$ W "noise level"
Agilent <a href="http://www.home.agilent.com">www.home.agilent.com</a>	W8486A	Power	75 – 110 GHz*	WR-10 waveguide (1.27 x 2.54 mm)	0.45 $\mu$ W "Meas. Noise"
Tydex <a href="http://www.tydexoptics.com/en">www.tydexoptics.com/en</a>	GC-1P Golay cell	Power (Golay cell)	0.04 – 15 THz	Free space 6 mm diam.	0.14 nW/Hz <sup>1/2</sup> "typ. NEP"
Gentec EO/Spectrum Detector <a href="http://www.gentec-eo.com">www.gentec-eo.com</a>	THz2I-BL-BNC pyroelectric	Power (pyroelectric)	0.1 – 30 THz	Free space 2 mm diam.	0.4 nW/Hz <sup>1/2</sup> "NEP"
Spiricon/Ophir <a href="http://www.ophiropt.com">www.ophiropt.com</a>	Pyrocam III	Power distribution (pyroelectric array)	0.1 – 280 THz	Free space 12.4 x 12.4 mm	45 nW/Hz <sup>1/2</sup> /pixel "NEP"
AB Millimetre <a href="http://www.abmillimetre.com">www.abmillimetre.com</a>	MVNA-8-350	VNA	0.008 – 1.0 THz	Single-mode wave- guide (banded)	80 dB @ 900GHz dynamic range
OML*** <a href="http://www.omlinc.com">www.omlinc.com</a>	VxxVNA2	VNA	50 – 500 GHz	Single-mode wave- guide (banded)	75 dB @ 300GHz 50 dB @ 500GHz dynamic range
VDI*** <a href="http://vadiodes.com/">http://vadiodes.com/</a>	WRxx	VNA	75 – 1050 GHz	Single-mode wave- guide (banded)	100 dB @ 650GHz dynamic range
RPG/Rohde&Schwarz*** <a href="http://www.radiometer-physics.de">www.radiometer-physics.de</a> <a href="http://www2.rohde-schwarz.com">www2.rohde-schwarz.com</a>	ZVA-xx	VNA	50 - 500 GHz	Single-mode wave- guide (banded)	70 dB @ 300 GHz dynamic range
Emcore <a href="http://www.emcorephotonicsystems.com">www.emcorephotonicsystems.com</a>	PB-7100	Spectrometer frequency-domain	0.1 – 1.9 THz	Free space	0.1 GHz resolution 80 dB SNR @200 GHz 60 dB SNR @1 THz
Toptica <a href="http://www.toptica.com">www.toptica.com</a>	THz-CW	Spectrometer frequency-domain	0.05 – 1.8 THz	Free space	0.1 GHz abs. accuracy, 1 MHz resolution 70 dB SNR @ 500 GHz
Teraview <a href="http://www.teraview.com">www.teraview.com</a>	CW-400	Spectrometer frequency-domain	0.05-1.5 THz	Free space	0.1 GHz resolution 50 dB SNR @ 500GHz
Picometrix <a href="http://www.picometrix.com">www.picometrix.com</a>	TRay-4000	Spectrometer time-domain	0.02 – 2 THz	Free space	2.8 ns scan range 70 dB SNR max
Teraview <a href="http://www.teraview.com">www.teraview.com</a>	TPS-3000	Spectrometer time-domain	0.06 – 3 THz	Free space	7.5 GHz resolution 70 dB SNR, 0.3-0.9THz
ZOmega <a href="http://zomega-terahertz.com">http://zomega-terahertz.com</a>	mini-Z	Spectrometer time-domain	0.1 – 4 THz	Free space	Resolution < 50 GHz 70 dB SNR at 0.5 THz

Note: Inclusion in this table in no way constitutes any form of endorsement of the instruments by the authors, by NIST, or by the Univ. of Colorado nor any claim that the instruments' quoted specifications are correct.

\* Quoted operating range, not range of calibration, except Agilent W8486A

\*\* Typical specification, quoted verbatim from datasheet or website.

\*\*\* Listed are manufacturers of the extender modules. In some cases these are distributed through manufacturers of the base VNA instrument.

for THz radiometry and power measurements that is based on blackbodies, and this has in fact been proposed at some national standard laboratories [11], [84], [110].

Table IV gives an overview of a number of commercially available instruments at the time of writing of this paper. This list is not intended to be complete, but is meant only to show some examples of the capabilities that are available. The comments in the table do not provide a complete description of the instruments, but are meant to provide examples of performance parameters. Very few of the instruments shown in Table IV can be directly compared. Though it is possible to use harmonic mixers for spectrum analysis, at this time no packaged spectrum analysis and noise measurement instruments are commercially available. On the other hand, FTIR spectrometers are not included here since they are a mature technology and we feel beyond the scope of this paper. The last several rows in Table IV refer to photonic-based commercial instruments. It should be pointed out that in the last five years, THz electronics has un-

dergone rapid development and growth, and this is reflected in Table IV, though historically photonics research has been quite active.

In the past, the limitations of THz metrology resulted from the available source power levels. Sources, amplifiers, multipliers, mixers, and detectors have improved to a point that their performance is not the main limiting factor in most basic measurements. Currently, measurement accuracy in state-of-the-art instruments is limited by interconnect quality, repeatability, and the lack of accepted standards.

As a final comment, much of the THz literature does not use SI units and standardized nomenclature. It is the hope of the authors that a new archival IEEE journal will contribute to propagating this important metrology aspect in the THz community. Appendix C in [54] ("An Antiquarian's Garden of Sane and Outrageous Terminology") provides a useful and entertaining insight into how results from different sources can be reconciled by agreeing on units and nomenclature.

## ACKNOWLEDGMENT

The authors are grateful to J. Hesler, R. Weikle, R. Wylde, W. Deal, P. Goy, C. Dietlein, and K. Vanhille for providing comments or unpublished information regarding their components and instruments. The second author is grateful to the DARPA THz Electronics program for support and to all its participants, particularly B. Wallace and D. Williams, for extensive discussions on THz metrology.

## REFERENCES

- [1] H. B. Wallace, "Analysis of RF imaging applications at frequencies over 100 GHz," *Appl. Opt.*, vol. 49, pp. E38–E47, 2010.
- [2] R. Appleby and H. B. Wallace, "Standoff detection of weapons and contraband in the 100 GHz to 1 THz region," *IEEE J. Antennas Propag.*, vol. 55, pp. 2944–2956, 2007.
- [3] Y. C. Shen, T. Lo, P. F. Taday, B. E. Cole, W. R. Tribe, and M. C. Kemp, "Detection and identification of explosives using terahertz pulsed spectroscopic imaging," *Appl. Phys. Lett.*, vol. 86, p. 241116, 2005.
- [4] P. F. Taday, "Applications of terahertz spectroscopy to pharmaceutical sciences," *Phil. Trans. R. Soc. Lond. A.*, vol. 362, pp. 351–364, 2004.
- [5] J. Zmuidzinis and P. L. Richards, "Superconducting detectors and mixers for millimeter and submillimeter astrophysics," *Proc. IEEE*, vol. 92, pp. 1597–1616, 2004.
- [6] D. Mittleman, *Sensing With Terahertz Radiation*. Berlin, Germany: Springer-Verlag, 2003.
- [7] E. N. Grossman, C. Dietlein, J. Ala-Laurinaho, M. Leivo, L. Gronberg, M. Gronholm, P. Lappalainen, A. Rautiainen, A. Tamminen, and A. Luukanen, "Passive terahertz camera for standoff security screening," *Appl. Opt.*, vol. 49, pp. E106–E120, 2010.
- [8] *Metrologia*. Sèvres, France: Bureau Internationale de Poids et Mesures, www.bipm.org.
- [9] B. N. Taylor and C. E. Kuyatt, "Guidelines for Evaluating and Expressing the Uncertainty of NIST Measurement Results," NIST, Technical Note 1297, 1994 [Online]. Available: <http://www.nist.gov/pml/pubs/tl1297/index.cfm>
- [10] J. J. O'Conner and E. F. Robertson, "The History of Measurement," 2003 [Online]. Available: <http://www-history.mcs.st-and.ac.uk/Hist-Topics/Measurement.html>
- [11] B. Gutschwager, C. Monte, H. Delsim-Hashemi, O. Grimm, and J. Hollandt, "Calculable blackbody radiation as a source for the determination of the spectral responsivity of THz detectors," *Metrologia*, vol. 46, pp. S165–S169, 2009.
- [12] M. Naftaly and R. Dudley, "Methodologies for determining the dynamic ranges and signal-to-noise ratios of terahertz time-domain spectrometers," *Opt. Lett.*, vol. 8, p. 1213, 2009.
- [13] J. L. Hesler and T. W. Crowe, "Responsivity and noise measurements of zero-bias Schottky diode detectors," presented at the 18th Int. Symp. Space Terahertz Technology (ISSTT), Pasadena, CA, Mar. 2007.
- [14] A. C. Young, J. D. Zimmerman, E. R. Brown, and A. C. Gossard, "Semimetal-semiconductor rectifiers for sensitive room-temperature microwave detectors," *Appl. Phys. Lett.*, vol. 87, p. 163506, 2005.
- [15] J. J. Lynch, J. N. Schulman, and P. H. Moyer, "Low noise direct detection sensors for millimeter wave imaging," in *Proc. IEEE Compound Semiconductor Integrated Circuit Symp. (CSIC 2006)*, 2006, pp. 215–218.
- [16] S. Komiyama, O. Astafiev, V. Antonov, T. Kutsuwa, and H. Hirai, "A single-photon detector in the far-infrared range," *Lett. Nature*, vol. 403, pp. 405–407, 2000.
- [17] M. McDonald and E. N. Grossman, "Niobium microbolometers for far-infrared detection," *IEEE Trans. Microw. Theory Tech.*, vol. 43, pp. 893–896, 1995.
- [18] A. Luukanen, E. N. Grossman, A. J. Miller, P. Helistö, J. S. Penttilä, H. Sipola, and H. Seppä, "An ultra-low noise superconducting antenna-coupled microbolometer with a room-temperature read-out," *IEEE Microw. Wireless Compon. Lett.*, vol. 16, pp. 464–466, 2006.
- [19] E. E. Haller, "Advanced far-infrared detectors," *Infrared Physics and Technology*, vol. 35, pp. 127–146, 1994.
- [20] D. Dooley, "Sensitivity of broadband pyroelectric terahertz detectors continues to improve," *Laser Focus World*, vol. 46, pp. 49–56, 2010.
- [21] MTI Instruments – Catalog [Online]. Available: <http://www.mtinstruments.com/thzdetectors>
- [22] W. Bishop, E. Meiburg, R. Mattauch, T. Crowe, and L. Poli, "A micron-thickness, planar Schottky diode chip for terahertz applications with theoretical minimum parasitic capacitance," in *IEEE MTT-S Int. Microwave Symp. Dig.*, 1990, vol. 3, pp. 1305–1308.
- [23] Agilent, "Agilent E4418B/E4419B EPM Series Power Meters and 8480 Power Sensors Datasheet," 2006.
- [24] J. Wei, D. Olaya, B. S. Karasik, S. V. Pereversev, A. V. Sergeev, and M. E. Gershonson, "Ultrasensitive hot-electron nanobolometers for terahertz astrophysics," *Nature Nanotechnol.*, vol. 3, pp. 496–500, 2008.
- [25] MTI Instruments – Catalog [Online]. Available: <http://www.mtinstruments.com/thzdetectors>
- [26] Virginia Diodes Inc. – Catalog [Online]. Available: <http://vadiodes.com/>
- [27] V. Radisic, K. Leong, X. Mei, S. Sarkozy, W. Yoshida, P.-H. Liu, J. Uyeda, R. Lai, and W. R. Deal, "A 50 mW 220 GHz power amplifier module," in *IEEE MTT-S Int. Microwave Symp. Dig.*, 2010, pp. 45–48.
- [28] E. R. Brown, K. A. McIntosh, K. B. Nichols, and C. L. Dennis, "Photomixing up to 3.8 THz in low-temperature-grown GaAs," *Appl. Phys. Lett.*, vol. 66, pp. 285–287, 1995.
- [29] J. E. Carlstrom, R. L. Plambeck, and D. D. Thornton, "A continuously tunable 65–115 GHz Gunn oscillator," *IEEE Trans. Microw. Theory Tech.*, vol. MTT-33, pp. 610–619, 1985.
- [30] T. Ishibashi, M. Ino, T. Makimura, and M. Ohmori, "Liquid-nitrogen cooled submillimeter silicon IMPATT diodes," *Electronics Lett.*, vol. 13, pp. 299–300, 1977.
- [31] J. Hesler *et al.*, "Fixed-tuned submillimeter wavelength waveguide mixers using planar Schottky-barrier diodes," *IEEE Trans. Microw. Theory Tech.*, vol. 45, pp. 653–658, 1997.
- [32] OML Inc. – Catalog [Online]. Available: <http://omlinc.com/>
- [33] W. Deal, "Solid-state amplifiers for terahertz electronics," in *IEEE MTT-S Int. Microwave Symp. Dig.*, 2010, pp. 1122–1125.
- [34] K. A. McIntosh, E. R. Brown, K. B. Nichols, O. B. McMahon, W. F. DiNatale, and T. M. Lyszczarz, "Terahertz measurements of resonant planar antennas coupled to low temperature grown GaAs photomixers," *Appl. Phys. Lett.*, vol. 69, p. 3632, 1996.
- [35] E. R. Brown, "THz generation by photomixing in ultrafast photoconductors," *Int. J. High-Speed Electronics and Systems*, vol. 13, pp. 497–545, 2003.
- [36] S. Roseau *et al.*, "Advances in high-power millimeter-wave grid array sources," in *Vacuum Electronics Int. Conf. Abstracts*, 2000, ISBN 0-7803-5987-9.
- [37] R. Hwu, L. Sadwick, N. Luhmann, D. Rutledge, M. Sokolic, and B. Hancock, "Quasi-optical watt-level millimeter-wave monolithic solid-state diode-grid frequency multipliers," in *IEEE MTT-S Int. Microwave Symp. Dig.*, 1989, vol. 3, pp. 1069–1067.
- [38] P. Siegel, P. Smith, M. Gaidis, and S. Martin, "2.5-THz GaAs monolithic membrane-diode mixer," *IEEE Trans. Microw. Theory Tech.*, vol. 47, pp. 596–604, 1999.
- [39] W. R. Deal, X. B. Mei, Radisic, W. Yoshida, P. H. Liu, J. Uyeda, M. Barsky, T. Gaier, A. Fung, L. Samoska, and R. Lai, "Demonstration of a S-MMIC LNA with 16-dB gain at 340-GHz," in *Compound Semiconductor Int. Conf.*, 2007, pp. 75–78.
- [40] W. Deal, X. B. Mei, V. Radisic, K. Leong, S. Sarkozy, B. Gorospe, J. Lee, P. H. Liu, W. Yoshida, J. Zhou, M. Lange, J. Uyeda, and R. Lai, "Demonstration of a 0.48 THz amplifier module using InP HEMT transistors," *IEEE Trans. Microw. Theory Tech.*, vol. 20, pp. 289–294, 2010.
- [41] I. R. Medvedev, M. Behnke, and F. C. DeLucia, "Fast analysis of gases in the submillimeter/terahertz with "absolute" specificity," *Appl. Phys. Lett.*, vol. 86, p. 154105, 2005.
- [42] M. van Exter, C. Fattering, and D. Grischkowsky, "High brightness terahertz beams with an ultrafast detector," *Appl. Phys. Lett.*, vol. 55, p. 337, 1989.
- [43] Custom Microwave Inc. – Catalog [Online]. Available: <http://www.custommicrowave.com/>
- [44] "Power Measurement Above 110 GHz," Virginia Diodes, Inc., Charlottesville, VA, Application Note VDI-704, 2007.
- [45] J. L. Doane, "Low loss propagation in corrugated rectangular waveguide at 1 mm wavelength," *Int. J. Infrared and Millimeter Waves*, vol. 8, pp. 13–27, 1987.
- [46] P. F. Goldsmith, *Quasioptical Systems*. New York: IEEE Press, 1998.
- [47] R. Wylde and D. H. Martin, "Gaussian beam-mode analysis and phase-centers of corrugated feed horns," *IEEE Trans. Microw. Theory Tech.*, vol. 41, pp. 1691–1699, 1993.
- [48] L. Hung, "Modal analysis and design of compound gratings and frequency selective surfaces," Ph.D. dissertation, Univ. of Colorado, Boulder, 2006.
- [49] D. Sherrer and J. Fisher, "Coaxial waveguide microstructures and the method of formation thereof," U.S. Patent 7 012 489, Mar. 14, 2006.
- [50] M. Lukic, S. Rondineau, Z. Popović, and D. S. Filipovic, "Modeling of realistic rectangular micro-coaxial lines," *IEEE Trans. Microw. Theory Tech.*, vol. 54, pp. 2068–2076, 2006.

- [51] J. E. A. Oliver, "A 3-D micromachined W-band cavity-backed patch antenna array with integrated rectacoax transition to waveguide," in *IEEE MTT-S Int. Microw. Symp. Dig.*, 2009, pp. 1641–1644.
- [52] L. Ranzani, N. Ehsan, and Z. Popović, "G-band frequency-scanned antenna arrays," in *Proc. Int. Symp. Antennas and Propag.*, 2010, pp. 1–4.
- [53] F. Hengstberger, *Absolute Radiometry*. San Diego, CA: Academic, 1989.
- [54] J. M. Palmer and B. G. Grant, *The Art of Radiometry*. Bellingham, WA: SPIE, 2010.
- [55] "Fundamentals of RF and microwave power measurements," Agilent, Appl. Note AN-1449-1, 2009.
- [56] J. J. Choi, A. H. McCurdy, F. N. Wood, R. H. Kyser, J. P. Calame, K. T. Nguyen, B. G. Danly, T. M. Antonsen, B. Levush, and R. K. Parker, "Experimental investigation of a high power, two-cavity, 35 GHz gyrokystron amplifier," *IEEE Trans. Plasma Sci.*, vol. 26, pp. 416–425, 1998.
- [57] M. Blank, B. G. Danly, B. Levush, P. E. Latham, and D. E. Pershing, "Experimental demonstration of a W-band gyrokystron amplifier," *Phys. Rev. Lett.*, vol. 79, pp. 4485–4488, 1997.
- [58] J. E. Martin, N. P. Fox, and P. J. Key, "A cryogenic radiometer for absolute radiometric measurements," *Metrologia*, vol. 21, pp. 147–155, 1985.
- [59] T. J. Quinn and S. E. Martin, "A radiometric determination of the Stefan-Boltzmann constant and thermodynamic temperatures between  $-40\text{ C}$  and  $+100\text{ C}$ ," *Phil. Trans. R. Soc. Lond.*, vol. 316, pp. 85–189, 1985.
- [60] T. J. Quinn and J. E. Martin, "Cryogenic radiometry, prospects for further improvements in accuracy," *Metrologia*, vol. 28, pp. 155–161, 1991.
- [61] D. A. Jennings and E. D. West, "A laser power meter for large beams," *Rev. Sci. Instr.*, vol. 41, pp. 565–567, 1970.
- [62] N. Erickson, "A fast and sensitive submillimeter waveguide power meter," in *Proc. 10th Int. Symp. Space Terahertz Technology*, 1999, vol. 10, pp. 501–507.
- [63] N. Erickson, "A fast, very sensitive calorimetric power meter for millimeter to submillimeter wavelengths," in *Proc. 13th Int. Symp. Space Terahertz Technology*, 2002, vol. 13, pp. 301–307.
- [64] N. Erickson, "Millimeter-Submillimeter Power Meter Operating Manual," Erickson Instruments, Amherst, MA, 2008.
- [65] D. G. Moss, J. R. Birch, D. H. Martin, and G. W. Poulson, "The absolute determination of near millimeter wave power in free space," in *Proc. 18th Eur. Microwave Conf.*, 1988, pp. 732–737.
- [66] T. Anbinderis, P. Anbinderis, A.-V. Usoris, P. Bagdonaite, E. Prusakova, I. Kasalynas, E. Sirmulis, D. Seliuta, and G. Valusis, "Waveguide-based calorimeter for terahertz frequency range," *Electronics Lett.*, vol. 43, no. 14, pp. 1–2, 2007.
- [67] A. N. Akhiezer, A. P. Senko, and V. P. Seredniy, "Millimeter wave power standards," *IEEE Trans. Instrum. Meas.*, vol. 46, pp. 495–498, 1997.
- [68] T. O. Klassen, J. N. Hovenier, J. Fischer, G. Jakob, A. Poglitsch, and O. Sternberg, "THz Calorimetry: An absolute power meter for terahertz radiation and the absorptivity of the Herschel Space Observatory telescope mirror coating," in *Proc. SPIE*, 2004, vol. 5354, pp. 159–167.
- [69] D. W. Allen, "Statistics of atomic frequency standards," *Proc. IEEE*, vol. 54, pp. 221–230, 1966.
- [70] D. W. Allen, "Should the classical variance be used as a basic measure in standards metrology?," *IEEE Trans. Instrum. Meas.*, vol. IM-36, pp. 646–654, 1987.
- [71] G. Rau, R. Schieder, and B. Vowinkel, "Characterization and measurement of radiometer stability," presented at the 14th Eur. Microwave Conf., Liege, Belgium, 1984.
- [72] J. W. Kooi, G. Chattopadhyay, M. Thielman, T. G. Phillips, and R. a. Schieder, "Noise stability of SIS receivers," *Int. J. IR and Mm Waves*, vol. 21, pp. 689–716, 2000.
- [73] V. Vasic, D. G. Feist, S. Muller, and N. Kampfer, "An airborne radiometer for stratospheric water vapor measurements at 183 GHz," *IEEE Trans. Geosci. Remote Sens.*, vol. 43, pp. 1563–1570, 2005.
- [74] J. Randa, J. Lahtinen, A. Camps, A. Gasiewski, M. Hallikainen, D. M. LeVine, M. Martin-Neira, J. Piepmeier, P. W. Rosenkranz, C. S. Ruf, J. Shiue, and N. Skou, "Recommended terminology for microwave radiometry," NIST Technical Note 1551, pp. 1–31, 2008.
- [75] C. D. Reintsema, J. A. Koch, and E. N. Grossman, "High precision electrical substitution radiometer based on superconducting resistive transition-edge thermometry," *Rev. Sci. Instr.*, pp. 152–163, 1998.
- [76] J. Hesler, A. R. Kerr, W. Grammer, and E. Wollack, "Recommendations for waveguide interfaces to 1 THz," in *Proc. 18th Int. Symp. Space Terahertz Technology*, 2007, pp. 1–4.
- [77] Y. S. Lau and A. Denning, "An innovative waveguide interface for millimeter wave and submillimeter wave applications," presented at the 69th ARFTG Conf., Honolulu, HI, 2007.
- [78] H. Li, A. R. Kerr, J. Hesler, H. Xu, and R. M. Weikle, "A ring-centered waveguide flange for millimeter- and submillimeter-wave applications," presented at the IEEE Int. Microwave Symp., Anaheim, CA, 2010.
- [79] J. B. Fowler, R. S. Duruvasula, and A. C. Parr, "High-accuracy aperture-area measurement facilities at the National Institute of Standards and Technology," *Metrologia*, vol. 35, pp. 496–500, 1998.
- [80] W. R. Blevin, "Diffraction losses in radiometry and photometry," *Metrologia*, vol. 6, p. 39, 1970.
- [81] P. Edwards and M. McCall, "Diffraction loss in radiometry," *Appl. Opt.*, vol. 42, pp. 5024–5032, 2003.
- [82] A. C. Parr, "A national measurement system for radiometry, photometry, and pyrometry based upon absolute detectors," National Institute of Standards and Technology (NIST), Gaithersburg, MD, Jul. 18, 2007 [Online]. Available: <http://physics.nist.gov/Pubs/TN1421/contents.html>
- [83] D. Adamson, N. Ridler, and J. Howes, "Recent and future developments in millimetre and sub-millimetre wavelength measurement standards at NPL," presented at the 5th ESA Workshop on Millimetre Wavelength Technology and Applications, Noordwijk, The Netherlands, 2009.
- [84] L. Werner, H.-W. Hubers, P. Meindl, R. Muller, H. Richter, and A. Steiger, "Towards traceable radiometry in the terahertz region," *Metrologia*, vol. 46, pp. S160–S164, 2009.
- [85] J. C. Mather, D. J. Fixsen, R. A. Shafer, C. Mosier, and D. T. Wilkonson, "Calibrator design for the COBE far infrared absolute spectrophotometer (FIRAS)," *Astrophys. J.*, vol. 512, pp. 511–520, 1999.
- [86] H. Hemmati, J. C. Mather, and W. L. Eichorn, "Submillimeter and millimeter wave characterization of absorbing materials," *Appl. Opt.*, vol. 24, pp. 4489–4492, 1985.
- [87] R. H. Giles, A. J. Gatesman, J. Fitzgerald, S. Fisk, and J. Waldman, "Tailoring artificial dielectric materials at terahertz frequencies," in *Proc. 4th Int. Symp. Space Terahertz Technology*, Los Angeles, CA, Apr. 1993.
- [88] A. Lonnqvist, A. Tamminen, J. Mallat, and A. Raisanen, "Monostatic reflectivity measurement of radar absorbing materials at 310 GHz," *IEEE Trans. Microw. Theory Tech.*, vol. 54, pp. 3486–3491, 2006.
- [89] A. Tamminen, A. Lonnqvist, J. Mallat, and A. Raisanen, "Monostatic reflectivity and transmittance of radar absorbing materials at 650 GHz," *IEEE Trans. Microw. Theory Tech.*, vol. 56, pp. 632–637, 2008.
- [90] J. Saily and A. Raisanen, "Characterization of submillimeter wave absorbers from 200–600 GHz," *Int. J. IR and Mm Waves*, vol. 25, pp. 71–89, 2004.
- [91] T. O. Klaassen, J. H. Blok, J. N. Hovenier, G. Jakob, D. Rosenthal, and K. J. Wildeman, "Absorbing coatings and diffuse reflectors for the Herschel platform submillimeter spectrometers HIFI and PACS," in *Proc. SPIE, IR Space Telescopes and Instruments*, 2002, vol. 4850, pp. 788–791.
- [92] P. H. Siegel, R. H. Tuffias, and P. Goy, "A simple millimeter-wave blackbody load," in *Proc. 9th Int. Conf. Space THz Technology*, 1998, pp. 1–10.
- [93] B. Carli, "Design of a blackbody reference standard for the submillimeter region," *IEEE Trans. Microw. Theory Tech.*, vol. MTT-22, pp. 1094–1099, 1974.
- [94] A. Murk, R. Wylde, R. Spurrett, P. Furholz, and N. Kampfer, "Blackbody calibration targets with ultralow reflectivity at submillimeter wavelengths," presented at the 4th ESA Workshop on Millimetre-Wave Technology and Applications, Espoo, Finland, 2006.
- [95] C. R. Dietlein, Z. Popović, and E. N. Grossman, "Aqueous blackbody calibration source for millimeter-wave/terahertz metrology," *Appl. Opt.*, vol. 47, pp. 5604–5615, 2008.
- [96] P. Goy and M. Gross, "Millimeter and sub-millimeter network vector analyzer," U.S. Patent 5,119,035, 1992, French Patent, 1989.
- [97] P. Goy and M. Gross, "Millimeter and submillimeter network vector analyzer," Eur. Patent EP0420767, 1991.
- [98] P. Goy, M. Gross, and S. Caropen, "Millimeter-wave and submillimeter wave vector network analyzer up to 1000 GHz; basic principles and applications," presented at the 4th Int. Conf. Millimeter and Submillimeter Waves and Applications, San Diego, CA, 1998.
- [99] T. Reck, L. Chen, C. Zhang, C. Groppi, H. Xu, A. Arsenovic, N. S. Barker, A. W. Lichtenberger, and R. M. Weikle, "Micromachined on-wafer probes," in *IEEE MTT-S Int. Microwave Symp. Dig.*, 2010, pp. 6568–6571.

- [100] H. Li, A. R. Kerr, J. L. Hesler, G. Wu, Q. Yu, N. S. Barker, and R. M. Weikle, II, "An improved ring-centered waveguide flange for millimeter- and submillimeter-wave applications," presented at the 76th ARFTG Microwave Measurement Symp., Clearwater Beach, FL, 2010.
- [101] D. F. Williams, "500 GHz–750 GHz rectangular-waveguide vector-network-analyzer calibrations," *IEEE Trans. Terahertz Sci. Technol.*, vol. 1, no. 2, Nov. 2011.
- [102] U. Gaertner, B. Schiek, and O. Ostwald, "Homodyne network analyzer with cascaded digital phase shifters," *Proc. IEEE*, vol. 74, pp. 66–68, 1986.
- [103] Y. Zhang, G. Colef, Y. Li, and G. Eichmann, "Six-port optical reflectometer," *IEEE Trans. Instrum. Meas.*, vol. 40, pp. 869–871, 1991.
- [104] S. W. Ulker and R. M. , II, "A sampled-line reflectometer for submillimeter-wave measurements," in *IEEE MTT-S Int. Microwave Symp. Dig.*, 2002, pp. 1677–1680.
- [105] G. M. Rebeiz, "Millimeter wave and THz integrated circuit antennas," *Proc. IEEE*, vol. 80, pp. 1748–1770, 1992.
- [106] C. R. Dietlein, J. D. Chisum, M. V. Ramíz, A. Luukanen, E. N. Grossman, and Z. Popović, "Integrated microbolometer antenna characterization from 95–650 GHz," in *IEEE MTT-S Int. Microwave Symp. Dig.*, 2007, pp. 1165–1168.
- [107] P. Goy, S. Caroopen, and M. Gross, "Vector characterization of millimeter-submillimeter antennas with a single setup in the 8–1000 GHz interval," presented at the Int. Conf. Antenna Technologies, Ahmedabad, India, 2005.
- [108] G. Junkin, T. Huang, and J. C. Bennett, "Holographic testing of terahertz antennas," *IEEE Trans. Antennas Propag.*, vol. 48, pp. 409–417, 2000.
- [109] E. N. Grossman, A. Luukanen, and A. J. Miller, "Holographic microantenna array metrology," in *Proc. SPIE, Passive Millim.-Wave Imag. Technol. VIII*, 2005, vol. 5789, pp. 44–50.
- [110] J. W. Lamb, "Miscellaneous data of materials for millimetre and submillimetre optics," *Int. J. IR and MM Waves*, vol. 17, pp. 1997–2034, 1996.



**Zoya Popović** (S'86–M'90–SM'99–F'02) received the Dipl.Eng. degree from the University of Belgrade, Serbia, Yugoslavia, in 1985, and the Ph.D. degree from the California Institute of Technology, Pasadena, in 1990.

Since 1990, she has been with the University of Colorado at Boulder, where she is currently a Distinguished Professor and holds the Hudson Moore Jr. Chair in the Department of Electrical, Computer and Energy Engineering. In 2001, she was a Visiting Professor with the Technical University of Munich, Mu-

nich, Germany. Since 1991, she has graduated 40 Ph.D. students. Her research interests include high-efficiency, low-noise, and broadband microwave and millimeter-wave circuits, quasi-optical millimeter-wave techniques for imaging, smart and multibeam antenna arrays, intelligent RF front-ends, and wireless powering for batteryless sensors.

Prof. Popović was the recipient of the 1993 and 2006 Microwave Prizes presented by the IEEE Microwave Theory and Techniques Society (IEEE MTT-S) for the best journal papers, and received the 1996 URSI Issac Koga Gold Medal. In 1997, Eta Kappa Nu students chose her as a Professor of the Year. She was the recipient of a 2000 Humboldt Research Award for Senior U.S. Scientists from the German Alexander von Humboldt Stiftung. She was elected a Foreign Member of the Serbian Academy of Sciences and Arts in 2006. She was also the recipient of the 2001 Hewlett-Packard (HP)/American Society for Engineering Education (ASEE) Terman Medal for combined teaching and research excellence.



**Erich N. Grossman** (M'88–SM'06) received the A.B. degree in physics from Harvard College, Cambridge, MA, in 1980, and the Ph.D. degree in physics from the California Institute of Technology, Pasadena, CA, in 1987. His thesis work involved development of an ultra-low noise, heterodyne receiver for 2 THz astronomy.

From 1988 to 1989, he was a postdoctoral fellow at the University of Texas at Austin, and in 1989, he joined the National Institute of Standards and Technology (NIST), Boulder, CO, where he is now a physicist in the Optoelectronics Division. His work at NIST focuses on infrared and submillimeter system development. His notable accomplishments include the development and demonstration of the world's highest frequency, high efficiency lithographic antennas, the world's highest frequency Josephson junctions (awarded a Department of Commerce Gold Medal in 1993), and conception and early development of the SQUID multiplexer, first enabling large monolithic arrays of superconducting detectors. More recently, he has developed several 0.1–1 THz cameras for security applications. He is chair of the Metrology Working Group for the DARPA Terahertz Electronics program, and received the 2010 Allen V. Astin Measurement Science Award.